https://doi.org/10.33271/nvngu/2024-2/104

O. S. Beshta[1],
orcid.org/0000-0002-4648-0260,
O. O. Beshta[1],
orcid.org/0000-0001-6397-3262,
S. S. Khudolii[1],
orcid.org/0000-0003-2342-1556,
T. O. Khalaimov[*1],
orcid.org/0000-0002-0171-8503,
V. S. Fedoreiko[2],
orcid.org/0000-0001-5822-3002

1 – Dnipro University of Technology, Dnipro, Ukraine
2 – Ternopil Volodymyr Hnatiuk National Pedagogical University, Ternopil, Ukraine
* Corresponding author e-mail: khalaimov.ta.o@nmu.one

ELECTRIC VEHICLE ENERGY CONSUMPTION TAKING INTO ACCOUNT THE ROUTE TOPOLOGY

Purpose. Determining the impact of the route topology factor on the costs of mechanical work of an electric vehicle is the main task of this work. The impact is determined by calculating the costs of mechanical work during the movement of an electric vehicle, taking into account energy recovery. The task also includes assessment of the forces acting on an electric vehicle using the example of the 2014 Nissan Leaf AZEO.

Methodology. The paper uses a mathematical model that estimates the amount of mechanical work required to overcome one of the chosen routes, taking into account energy recovery. Evaluation is performed using the most common standardized cycle WLTC class 3b.

Findings. The result of the research is a developed mathematical model that will allow one to effectively estimate the amount of mechanical work to overcome the given route and the possible recovery energy. The proposed method makes it possible to determine the most economical route from the starting point to the destination, taking into account the cost of mechanical energy.

Originality. A description of the main components affecting the consumption of electricity is given, taking into account the full picture of the forces acting on the electric vehicle during movement.

Practical value. The obtained results are of practical importance for choosing the most optimal route of the electric vehicle, which contributes to the efficient use of energy. The proposed technique can be used in practice to plan routes from the point of view of maximum energy recovery.

Keywords: *electric vehicle, route topology, energy recovery, optimal route, energy efficiency, WLTC*

Introduction. The purpose of this study is to evaluate how the topology affects the mechanical energy consumption of the 2014 Nissan Leaf AZEO electric vehicle during operation, taking into account the complex of forces that act on it during movement and its ability to recover energy mode. Through the use of a mathematical model, the purpose is to measure the potential mileage on a single charge of an electric vehicle through various alternative routes with the intention of determining the most energy-efficient option.

As a result of this study, a mathematical model was developed, which allows estimating the mechanical work required for the passage of specific routes, including energy recovery according to the standardized WLTC class 3b cycle. The proposed computational approach facilitates the selection of a route to reach the destination by determining the most energy-efficient one.

The study outlines the main factors affecting electricity consumption, taking into account the whole spectrum of forces acting on an electric vehicle during operation. Using a mathematical model, the influence of the topology on the mechanical energy consumption of the 2014 Nissan Leaf AZEO was evaluated by determining the average mechanical resistance force relative to the angle of inclination of the road. In addition, the work required to overcome two alternative routes was calculated, taking into account the energy recovery mode.

Literature review. Electric vehicles (EVs) are divided into battery electric vehicles, fuel cell electric vehicles and extended range electric vehicles, which use a secondary power source either to charge the battery or to power the power plant – an electric machine.

Compared to conventional combustion engine vehicles, electric vehicles produce fewer emissions, are more efficient, and produce less noise. However, all-electric vehicles currently face significant challenges, including battery size and weight, short range on a single charge, and long charging times [1, 2]. All this creates significant obstacles for the widespread adoption of electric vehicles.

The main components of the electric vehicle transmission are the electric machine, the electric control unit, the battery, the battery management system, the DC/AC inverter, the DC/DC converter and the regenerative braking system. The traction electric motor is controlled by an electric control unit. It receives signals from the driver via the accelerator pedal, brake pedal, etc., as well as feedback signals from sensors, such as the speed and acceleration of the electric vehicle.

The regenerative braking system is designed to utilize most of the braking kinetic energy that occurs when the brake pedal is pressed.

Regenerative braking and frictional braking are usually used in electric vehicles. When deceleration is not usually abrupt, electric regenerative braking is used. Friction brakes are used for the sharpest decelerations. The interaction of recuperation and friction braking occurs under the influence of the control unit and this interaction is different for different types of electric vehicles [3]. The possibility of recuperating braking energy is a good feature of motor vehicles with electric traction, because it allows you to effectively use the resulting conversion of kinetic braking energy into electric energy to increase the mileage of electric vehicles on one battery charge [4, 5].

The influence of various factors on the process of recuperating braking. The recuperation process takes place in an electric vehicle exclusively in the braking mode, when the necessary reduction of the electric machine's power supply voltage from the AC/DC inverter in relation to its EMF leads to a change in the direction of the current.

Since braking occurs after a certain acceleration, the electric drive of an electric vehicle has a speed and current control system that ensures the stability of the dynamic moments of acceleration and braking at the level specified by the driver. Thus, the level of recuperation energy depends on the dynamic modes of motion of the electric vehicle. In this connection, there is a problem of taking into account the recovery energy to increase the inter-charge cycle of the battery, since the dynamics of traffic depends on many factors.

To determine the amount of fuel consumed, as well as greenhouse gas emissions in the world, a number of standardized tests are used, which are carried out on a dynamometric installation. One of the most common are The Worldwide harmonized Light vehicles Test Cycles (WLTC) [6, 7], cycles, which are intended for light vehicles and are used in particular to evaluate the consumption of electricity by electric vehicles. The WLTC cycles are part of the Worldwide harmonized Light vehicles Test Procedures (WLTP) published in Global technical regulation No 15 (GTR 15) [8], which is an agreement to introduce global technical regulations for wheeled vehicles, items of equipment and parts that can be installed and/or used on wheeled vehicles.

Currently, the following standardized cycles are used in the world to estimate fuel consumption, the level of CO_2 emissions, as well as mathematical modeling of the processes occurring in vehicles: NEDC UDDS; HWFET; UDDS; FTP; WLTP, WLTC, etc.

Estimation of energy consumption for the movement of an electric vehicle occurs in different ways. Analyzing the scientific literature, the authors [9] classified the methods for calculating the energy consumption of electric vehicles into three main categories: 1) analytical; 2) statistical; 3) computing based on artificial neural networks. In [9], it is stated that analytical models are based on vehicle dynamics along its path and transmission efficiency and can be used to estimate energy consumption during a trip for eco-route planning. Statistical models are based on real-world driving data to understand and derive empirical relationships between the energy consumption of an electric vehicle and various factors affecting its consumption. Computational models based on artificial neural networks were created to estimate the relationship between the energy consumption of an electric vehicle and the factors affecting consumption.

In the article [9], a mathematical model created by Simscape tools in MATLAB, combined with New European Driving Cycle (NEDC) test cycles, is also used to solve the issue of replacing a classic internal combustion engine (ICE) to an electric motor (EV). According to the results of the study, it turned out that such a replacement leads to a significant reduction in fuel consumption, which makes the system using EV 15–19 % more efficient. The NEDC cycle is used for the calculation for both proposed systems based on different types of engines, which is appropriate because the standardized cycles serve as a universal means of estimating energy consumption for passenger vehicles.

In the work [10], they dealt with the issue of designing electric machines for electric vehicles based on driving schedules. The UDDS and HWFET cycles were chosen to simulate typical urban traffic conditions. UDDS simulates a typical driving cycle within the city limits of a passenger vehicle that moves at relatively low speeds of 25–60 km/h. According to the article, this mode results in a significant amount of regenerative braking power due to many decelerations. The HWFET loop has only a few delays, which provide low regenerative braking power relative to the UDDS. In turn, the US06 cycle includes sharp accelerations and decelerations, as well as a high-speed cruising course during the cycle (the average speed is – 77.9 km/h). The authors of the article claim that the proposed mathematical vehicle model based on the Nissan Leaf's 80kW IPM machine provides a useful approach for estimating the instantaneous power and energy consumption of an electric vehicle with different designs of electric machines. The application of different driving cycles (UDDS, HWFET, US06) in the model makes it possible to investigate how changes in driving conditions (motion tachograms) contribute to the use of different types of machine designs and how they can be modified in order to increase the range of an electric vehicle.

In the article [11], a simplified mathematical model of the powertrain for the electric vehicle Nissan Leaf 2012 was developed using roll parameters, published by the Environmental Protection Agency (EPA), for modeling vehicle loads and using data from Argonne National Laboratory (ANL) to validate the model needed to calculate energy for traction and braking. Model results are compared with experimental UDDS data published by ANL. The model assumes that all available regenerative energy is returned to the battery if the regenerative power level is 20 kW or less. The authors demonstrated a high correlation, within 1–3 %, between model predictions and experimental data regarding: range, fuel economy, and fuel consumption predictions.

Purpose. Thus, the analysis of the literature showed that most researchers consider the issue of energy consumption of electric vehicles from the point of view of its evaluation and improvement of the efficiency of energy use. However, there is another factor that should be taken into account for the analysis of energy efficiency and prolongation of the inter-charge cycle of an electric vehicle – the effect of the recuperation process.

The effect of the recuperation process can play a significant role in the operation of an electric vehicle such as an electric car with significant fluctuations in the height of ascent and descent along the route of movement. With a limited range on one charge and a long charging time, the topology of the route will critically influence its choice from one charging station to another.

Compared to what has already been done in the world, this paper proposes a mathematical model for predicting the costs of mechanical work in order to choose a more energy-efficient route among several possible options, taking into account the topology of the area.

Methods. ***Mechanical traction force and resistance forces of an electric vehicle.*** The mechanical power of an electric vehicle is determined in the same way as for a conventional vehicle, namely, with the help of the resulting forces acting on its wheels when moving at a constant speed (cruise mode), acceleration (acceleration mode), braking (braking mode), in the direction of movement while ensuring the stability of the electric vehicle on the road [9, 12]. At the same time, the stability of the electric vehicle is ensured by the zero resultant component of the moments of forces that arise relative to the height of the center of gravity of the support points of the front and rear wheels when moving uphill or downhill [13, 14]. At the same time, in this case, the stability of the electric vehicle on the road when entering a turn is not considered.

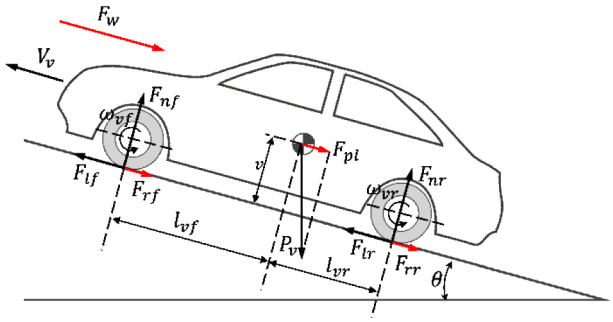

Fig. 1. The load on the electric vehicle when moving uphill

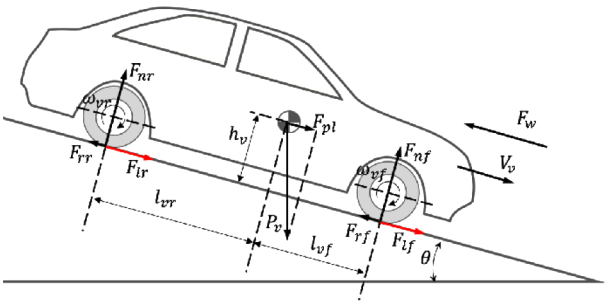

Fig. 2. The load on an electric vehicle when it is moving downhill

In accordance with these conditions, consider the following picture of the forces acting on the electric vehicle when it moves up (Fig. 1).

Definition of forces, geometric dimensions and other variables of Fig. 1 is presented in Table 1.

For the movement of an electric vehicle downhill, the picture of the distribution of operating forces is presented in Fig. 2.

Maximum mechanical traction force. According to Figs. 1 and 2, the maximum possible mechanical traction force F_t, which ensures the movement of the electric vehicle, consists of the traction force of the front F_{lf} and rear F_{lr} wheels

$$F_t = F_{lf} + F_{lr}; \tag{1}$$

$$F_{lf} = \mu_f F_{nf}; \tag{2}$$

$$F_{lr} = \mu_r F_{nr}, \tag{3}$$

where μ_f, μ_r are the friction coefficients for the front and rear wheels, respectively.

In general, $\mu_f \neq \mu_r$, but if we do not take into account slippage, then these coefficients can be considered equal (1–3). According to [12], the ranges of changes in friction coefficients are determined by climatic conditions and slip coefficients of the front s_f and rear s_r wheels. If we consider the radii r_d and angular velocities ω_v of the front and rear wheels to be the same, then the slip coefficients will also be the same and will be determined as.

Table 1

Definition of variables

	Definition
P_v	Vehicle mass
h_v	The height of the center of gravity of the vehicle
l_{vf}	The distance between the front axle and the center of gravity of the vehicle
l_{vr}	The distance between the rear axle and the center of gravity of the vehicle
V_v	Vehicle speed
F_w	Aerodynamic resistance
F_{nf}	Normal force on the front tires
F_{nr}	Normal power on the rear tires
F_{lf}	Longitudinal traction forces on the front tires
F_{lr}	Longitudinal traction forces on the rear tires
F_{pl}	Rolling power
F_{rf}	Friction resistance of the front wheels
F_{rr}	Friction resistance of the rear wheels
θ	Angle of inclination of the road
ω_{vf}	Angular speed of the front wheels
ω_{vr}	Angular speed of the rear wheels

$$s_v = \frac{r_d\omega_v - V_v}{r_d\omega_v}. \tag{4}$$

Then, according to [12], when $s_v < 0.2$, (4) the ranges of changes and the average value of the friction coefficient depending on climatic conditions can be presented in Table 2.

The normally acting forces of the front F_{nf} and rear F_{nr} wheels included in formulas (2, 3) are determined by the zero resultant moments of the forces acting with the shoulders relative to the support points of the front and rear wheels when moving uphill or downhill [12]. When moving up we have.

$$F_{nf} = \frac{-F_w h_w - F_{pl} h_v + P_v \cos(\theta) l_{vr} - (m_v a_v) h_v}{l_{vf} + l_{vr}}; \tag{5}$$

$$F_{nr} = \frac{F_w h_w + F_{pl} h_v + P_v \cos(\theta) l_{vf} + (m_v a_v) h_v}{l_{vf} + l_{vr}}. \tag{6}$$

When moving downhill

$$F_{nf} = \frac{-F_w h_w + F_{pl} h_v + P_v \cos(\theta) l_{vr} + (m_v a_v) h_v}{l_{vf} + l_{vr}}; \tag{7}$$

$$F_{nr} = \frac{F_w h_w - F_{pl} h_v + P_v \cos(\theta) l_{vf} - (m_v a_v) h_v}{l_{vf} + l_{vr}}. \tag{8}$$

The sum of forces according to formulas (5, 6) or (7, 8) determines the normal component of the electric vehicle's gravity.

$$F_{nf} + F_{nr} = P_v \cos(\theta), \tag{9}$$

where θ is the angle of inclination of the path surface.

Normal component of the electric vehicle's gravity determined by (9).

If the coefficients of friction for the front and rear wheels are equal $\mu_f = \mu_r = \mu$, we get the equation

$$F_t = \mu P_v \cos(\theta). \tag{10}$$

Equation: for determining the maximum mechanical traction force (10).

Resistance forces. ***Rolling resistance.*** The constantly acting force of resistance to the movement of an electric vehicle on the road is the force of resistance to rolling [15]. It occurs when the tires interact with the road surface. At the same time, a certain surface of interaction is created due to the crumpling of the tires under the weight of the electric vehicle, when the air

Table 2

The value of the coefficient of friction

Climatic conditions of the route	$\mu_{f/r}$	Average value
Normal	0.9–1.0	0.95
Rain	0.65–0.85	0.75
Snow	0.275–0.3	0.29
Ice	0.09–0.11	0.1

pressure in the front part of the tire is greater than in the rear part. This effect actually shifts the normal pressure force on the wheel F_n relative to the theoretical point of resistance by the amount b (Fig. 3).

$$F_r = F_n \xi_r \cos(\theta), \tag{11}$$

where $\xi_r = b/r_d$; r_d is the effective radius of the wheel.

Thus, the amount of normal pressure at the theoretical point of contact will decrease by the amount of $\cos(\theta)$, and the rolling resistance force F_r (11) will be determined by the rolling resistance coefficient ξ_r [12].

$$F_r = F_{rf} + F_{rr} = (F_{nf}\xi_{rf} + F_{nr}\xi_{rr}) \cos(\theta). \tag{12}$$

Accordingly, for an all-wheel drive electric vehicle, we have the total rolling resistance from the front axle F_{rf} and the rear axle F_{rr} of the wheels, taking into account that the coefficient ξ_r is different for the front and rear axles (12).

Air resistance. The force of air resistance occurs during the movement of an electric vehicle in any case, since there is an opposite movement of air in relation to the vehicle at the same speed. The presence of wind speed [9] increases or decreases the drag force depending on the direction of the wind.

$$F_w = \frac{1}{2}\rho S_{ve} C_d (V_v + V_w)^2, \tag{14}$$

where $\rho = 1.276$ kg/m^3 – air density; S_{ve} – the effective frontal area of the electric vehicle, m^2; $C_d = 0.24$–0.31 – the coefficient of aerodynamic resistance of a modern car; V_w – wind speed.

The general formula (14) that takes into account the effect of air resistance has the form [12, 13].

Rolling power. The rolling force is the force of motion resistance only in the case of the electric vehicle moving upwards. This force is the horizontal component of the machine's gravity in relation to the trajectory of movement and depends on the angle of inclination of the path.

$$F_{pl} = P_v \sin(\theta). \tag{15}$$

The rolling force is determined by the equation (15).

In the case of an electric vehicle moving downhill, the rolling force becomes the driving force and helps the movement.

Mechanical traction force to provide acceleration. According to Newton's second law, the acceleration of any physical body is determined by the resultant forces acting on it [16]. Accordingly, for the movement of an electric car with acceleration:

- uphill

$$F_t - F_{pl} - F_w - F_r = m_v a_v; \tag{16}$$

- downhill

$$F_t + F_{pl} - F_w - F_r = m_v a_v, \tag{17}$$

where a_v is acceleration; $m_v = P_v/g$ – mass of the electric vehicle; $g = 9.81$ m/s^2.

Conditions for providing the necessary mechanical traction force. Acceleration according to equations (16 and 17) is possible only under the condition that the mechanical traction force according to these formulas does not exceed the maximum traction force according to formula (10), i.e.

$$\mu P_v \cos(\theta) \geq F_{pl} + F_w + F_r + m_v a_v. \tag{18}$$

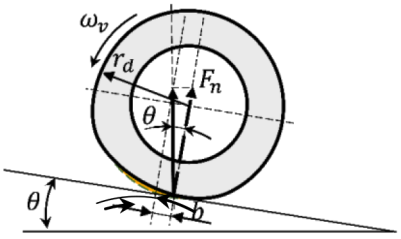

Fig. 3. Tire rolling resistance

Taking into account the formulas (13–15), we have for driving uphill

$$\mu P_v \cos(\theta) \geq P_v \sin(\theta) + \frac{1}{2}\rho S_{ve} C_d (V_v + V_w)^2 + P_v \xi_r \cos(\theta)^2 + m_v a_v. \tag{19}$$

It is obvious that if the condition (19) is fulfilled for driving uphill, then for downhill movement, when the rolling force helps the movement, this condition is fulfilled all the more.

$$\mu F_n \geq P_v \sin(\theta) + \frac{1}{2}\rho S_{ve} C_d (V_v + V_w)^2 + F_n \xi_r \cos(\theta)^2 + m_v a_v, \tag{20}$$

where $F_n = F_{nf}$ – for the front axle; $F_n = F_{nr}$ – for the rear axle.

In the case when one of the bridges is the driving one, the condition for providing the necessary mechanical traction force worsens (20).

Work of mechanical traction force. From the previous considerations, it is clear that the mechanical traction force of an electric vehicle changes when the driving mode is changed [17, 18]. Moreover, cruise mode, acceleration or braking modes depend not only on the driver's driving style, but also on the infrastructure of the route (availability of traffic lights, roundabouts, intersections, pedestrian crossings, traffic jams, etc.) and its topology. To determine the influence of the route topology on the consumption of mechanical energy of the electric drive of an electric vehicle, we will consider in general the i^{th} segment of the route uphill (Fig. 4) and downhill (Fig. 5).

The notation for Figs. 4 and 5 is presented in Table 3.

According to Figs. 4, 5 and Table 3, the following equations can be written.

$$L_v^i = L_U^i + L_D^i; \tag{21}$$

$$L_U^i = L_{U(a)}^i + L_{U(s)}^i + L_{U(b)}^i; \tag{22}$$

$$L_D^i = L_{D(a)}^i + L_{D(s)}^i + L_{D(b)}^i; \tag{23}$$

$$L_{U(s)}^i = L_U^i - L_{U(a)}^i - L_{U(b)}^i; \tag{24}$$

$$L_{D(s)}^i = L_D^i - L_{D(a)}^i - L_{D(b)}^i. \tag{25}$$

The work of the mechanical traction force on the i^{th} segment of the route will consist of the sum of the work of the corresponding traction forces on all sections of the route, which are determined by formulas (21–25).

$$A_U^i = F_{tU(a)}^i L_{U(a)}^i + F_{t,U(s)}^i L_{U(s)}^i + F_{t,U(b)}^i L_{U(b)}^i; \tag{26}$$

$$A_D^i = F_{t,D(a)}^i L_{D(a)}^i + F_{t,D(s)}^i L_{D(s)}^i + F_{t,D(b)}^i L_{D(b)}^i; \tag{27}$$

$$A_v^i = A_U^i + A_D^i. \tag{28}$$

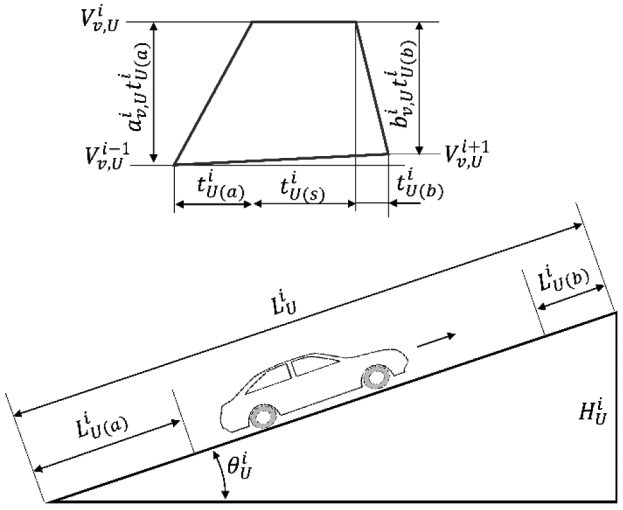

Fig. 4. A fragment of the route of the electric vehicle uphill

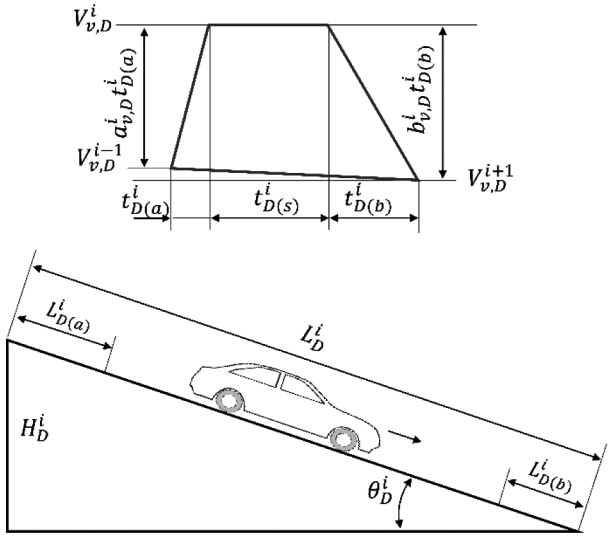

Fig. 5. A fragment of the route of the electric vehicle downhill

Table 3

Designation of the i^{th} segment of the route

L^i_U	The length of the route uphill
$L^i_{U(a)}$	The length of the route uphill with acceleration
$L^i_{U(b)}$	The length of the route uphill with braking
$L^i_{U(s)}$	The length of the cruise mode uphill
θ^i_U	Angle of rise
H^i_U	Height of rise
L^i_D	The length of the route downhill
$L^i_{D(a)}$	The length of the route downhill with acceleration
$L^i_{D(b)}$	The length of the route downhill with braking
$L^i_{D(s)}$	The length of the cruise mode downhill
θ^i_D	Angle of descent
H^i_D	Height of descent

If we assume that the values of accelerations and decelerations are constant, then we can present the segments of the route with acceleration and deceleration due to speeds (26–28).

$$L^i_{U(a)} = \frac{(V^i_{v,U})^2 - (V^{i-1}_{v,U})^2}{2a^i_{v,U}};$$

$$L^i_{U(b)} = \frac{(V^i_{v,U})^2 - (V^{i+1}_{v,U})^2}{2b^i_{v,U}};$$

$$L^i_{D(a)} = \frac{(V^i_{v,D})^2 - (V^{i-1}_{v,D})^2}{2a^i_{v,D}};$$

$$L^i_{D(b)} = \frac{(V^i_{v,D})^2 - (V^{i+1}_{v,D})^2}{2b^i_{v,D}},$$

where $a^i_{v,U}$, $a^i_{v,D}$ are acceleration on the i^{th} segment of the route on the ascent and descent, respectively; $b^i_{v,U}$, $b^i_{v,D}$ – deceleration on the i^{th} segment of the route on the ascent and descent, respectively; $V^{i-1}_{v,U}$ is the speed of the electric vehicle before climbing the i^{th} segment of the route; $V^i_{v,U}$ – the maximum speed of the electric vehicle after acceleration on a climb; $V^{i+1}_{v,U}$ is the speed of the electric vehicle after braking on a climb; $V^{i-1}_{v,D}$ is the speed of the electric vehicle at the beginning of the descent; $V^i_{v,D}$ – the maximum speed of the electric vehicle after acceleration on the descent; $V^{i+1}_{v,D}$ is the speed of the electric vehicle after braking on the descent – the initial speed of the next $i + 1$ segment of the route.

Traction forces included in equations (26–28) are described by formulas (13–17) taking into account the characteristics of each fragment on the i^{th} segment of the route

$$F^i_{tU(a)} = F^i_{pl,U} + F^i_{w,U(a)} + F^i_{r,U} + m_v a^i_{v,U};$$

$$F^i_{t,U(s)} = F^i_{pl,U} + F^i_{w,U(s)} + F^i_{r,U};$$

$$F^i_{t,U(b)} = F^i_{pl,U} + F^i_{w,U(s)} + F^i_{r,U};$$

$$F^i_{t,D(a)} = -F^i_{pl,D} + F^i_{w,D(a)} + F^i_{r,D} + m_v a^i_{v,D};$$

$$F^i_{t,D(s)} = -F^i_{pl,D} + F^i_{w,D(s)} + F^i_{r,D};$$

$$F^i_{t,D(b)} = -F^i_{pl,D} + F^i_{w,D(b)} + F^i_{r,D} - m_v b^i_{v,D}.$$

The forces of air resistance [19] during the period of acceleration and braking are taken into account by the average value of the speed on the corresponding sections of the route.

If the uphill route has a constant slope and consists of $n = a + s + b$ links, where a is the number of acceleration links; b – the number of deceleration links; s – the number of links with a constant speed, then the total mechanical work for uphill movement is determined by the following formulas

$$A_U = A^{pl}_U + A^r_U + A^w_U;$$

$$A^{pl}_U = P_v L_U \sin(\theta);$$

$$A^r_U = L_U \xi_r \cos(\theta)^2 + \sum_{i=1}^{a} a^i_{v,U} L^i_{U(a)};$$

$$A^w_U = \sum_{i=1}^{a} k^i_{w,U(a)} L^i_{U(a)} + \sum_{i=1}^{s} k^i_{w,U(s)} L^i_{U(s)} + \sum_{i=1}^{b} k^i_{w,U(b)} L^i_{U(b)},$$

where

$$k^i_{w,U(s)} = \frac{0.5\rho S_{ve} C_d}{P_v}(V^i_{v,U} + V_w)^2;$$

$$k^i_{w,U(a)} = \frac{0.5\rho S_{ve} C_d}{P_v}(0.5(V^{i-1}_{v,U} + V^i_{v,U}) + V_w)^2;$$

$$k^i_{w,U(b)} = \frac{0.5\rho S_{ve} C_d}{P_v}(0.5(V^i_{v,U} + V^{i+1}_{v,U}) + V_w)^2; \qquad L_U = \sum_{i=1}^{n} L^i_U.$$

Similarly, we obtain formulas for determining the mechanical work of an electric vehicle for downhill movement.

$$A_D = A^{pl}_D + A^r_D + A^w_D; \tag{29}$$

$$A^{pl}_D = -P_v L_D \sin(\theta); \tag{30}$$

$$A^r_D = L_D \xi_r \cos(\theta)^2 + \sum_{i=1}^{a} a^i_{v,D} L^i_{D(a)}; \tag{31}$$

$$A^w_D = \sum_{i=1}^{a} k^i_{w,D(a)} L^i_{D(a)} + \sum_{i=1}^{s} k^i_{w,D(s)} L^i_{U(s)} + \sum_{i=1}^{b} k^i_{w,D(b)} L^i_{D(b)}, \tag{32}$$

where

$$k^i_{w,D(s)} = \frac{0.5\rho S_{ve} C_d}{P_v}(V^i_{v,D} + V_w)^2;$$

$$k^i_{w,D(a)} = \frac{0.5\rho S_{ve} C_d}{P_v}(0.5(V^{i-1}_{v,D} + V^i_{v,D}) + V_w)^2;$$

$$k^i_{w,D(b)} = \frac{0.5\rho S_{ve} C_d}{P_v}(0.5(V^i_{v,D} + V^{i+1}_{v,D}) + V_w)^2; \qquad L_D = \sum_{i=1}^{n} L^i_D.$$

From formulas (29–32) it can be seen that there are certain components of mechanical work that depend on the angle of

the road slope. The change in the amount of mechanical work from the angle of inclination θ will be determined by derivatives.

$$dA_U/d\theta = L_U[P_v \cos(\theta) - \xi_r \sin(2\theta)];$$
$$dA_D/d\theta = -L_D[P_v \cos(\theta) + \xi_r \sin(2\theta)].$$

That is, it is possible to present a general formula for determining the mechanical work of an electric vehicle during ascent and descent through a constant component determined by horizontal movement and a variable component that depends on the angle of inclination of the road.

$$A_U = A_U(0) + A_U[\theta];$$
$$A_D = A_D(0) + A_D[\theta],$$

where $A_U[\theta] = (dA_U/d\theta)\theta$; $A_D[\theta] = (dA_D/d\theta)\theta$.

Mechanical energy consumption when using standard test cycles. Consider the standard WLTC test cycle, class 3b with the indicators presented in Fig. 6 and Table 4, and solve the following problems:

- to determine the impact of the slope of the route uphill and downhill on the consumption of mechanical energy of the electric vehicle;
- to determine the possible amount of mechanical energy that can be recovered during ascent and descent;
- to evaluate the possibilities of providing the necessary grip with the road when performing the WLTC class 3b test cycle when moving uphill.

We will solve the problems for the Nissan Leaf AZE0, 2014 electric vehicle with the parameters given in Table 4.

We accept the following initial conditions:

- maximum load of the electric vehicle;
- wind speed is zero;
- the coefficient of friction is the same on all wheels and is maximum;
- the coefficient of adhesion of the wheels to the road surface is the maximum for passenger vehicles produced;
- the test cycle is performed with a constant slope of the road either uphill or downhill;
- the route is straight and has no turns;
- the coefficient of aerodynamic resistance $C_d = 0.29$;
- the length of the route uphill is equal to the length of the route downhill, which makes it possible to compare energy consumption in both directions of movement.

The conditions for providing the required mechanical traction force in ideal dry weather at different angles of elevation are presented by calculations of the forces of movement resistance attributed to the weight of the Nissan Leaf AZE0 electric vehicle according to formula (20) in the form of Table 6. The "max" column shows the maximum possible traction force of the electric vehicle in relation to its weight for the given climatic conditions and the corresponding driving angle, and the other columns show the relative forces of movement resistance for different stages of the test cycle.

It can be seen from Table 6 that the execution of certain stages of the WLTP Class 3b cycle becomes impossible, starting from an uphill movement angle of 10°. An angle of 15° becomes critical for all stages, when the maximum possible traction force of the Nissan Leaf AZE0 electric vehicle becomes less than that necessary to overcome the resistance forces of movement. This does not at all mean that an electric vehicle cannot move at such an uphill slope, but it becomes impossible to provide the accelerations that are provided by the corresponding cycle requirements.

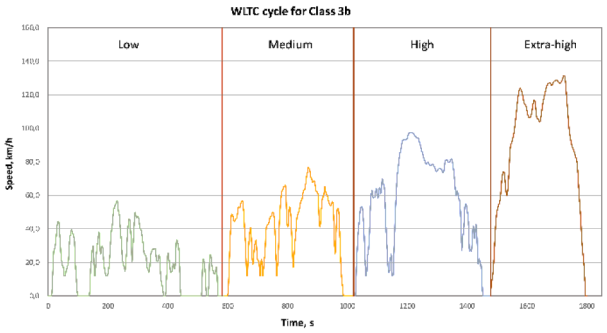

Fig. 6. Standard test cycle WLTC, class 3 [6]

Results. The results of calculations of the average mechanical force of resistance of the Nissan Leaf AZE0 electric vehicle when it moves in the WLTC, class 3b test cycle modes uphill and downhill in a straight line without the influence of wind, depending on the angle of the road, are presented in Table 7.

Negative signs in Table 7 represent the mechanical force that can be used as a source of recuperative energy to charge the battery.

The data in Table 7 are given for an electric vehicle without any load on board. To take into account the additional load, including the driver's weight, the data in Table 7 should be multiplied by the weight ratio of the loaded electric vehicle compared to the unloaded one.

The following conclusions can be drawn from the obtained data.

Obviously, this amount of energy cannot be recovered due to the limited power of the inverter and the speed of the battery charging process of this model of electric vehicle, as well as the lack of additional, fast means of receiving/giving up electrical energy, for example, supercapacitors.

It can be seen from the table that the values of the average movement resistance forces for different stages of the test cycle do not correspond to the meaning of this test stage. The names of the stages correspond to the level of maximum and average speed for the stage. Since this test cycle was created for vehicles with internal combustion engines, then, accordingly, the specific consumption of gasoline/diesel should be higher when the average speed increases. Since in this case we are talking only about the mechanical work of overcoming natural resistance forces without taking into account the energy losses for its transformation and transmission to the wheels, the main role here is played by the number of accelerations and decelerations and their level.

The data of mechanical resistance forces allow calculating the energy consumption of a route of any complexity from the point of view of topology. To do this, it is enough to decide on the mode of movement (Low, Middle, High, Extra-High) or adjacent (Low+Middle, High+Extra High, Total), choose a route with topological labels of height and length, which en-

Table 4

WLTP Class 3b cycle

Phase	Duration	Stop duration	Distance	p_{stop}	v_{max}	v_{ave} w/o stops	v_{ave} w/stops	a_{min}	a_{mac}
	s	s	m	%	km/h	km/h	km/h	m/s²	m/s²
Low 3	589	156	3,095	26.5	56.5	25.7	18.9	–1.47	1.47
Medium 3-2	433	48	4,756	11.1	76.6	44.5	39.5	–1.49	1.57
High 3-2	455	31	7,162	6.8	97.4	60.8	56.7	–1.49	1.58
Extra-High-3	323	7	8,254	2.2	131.3	94.0	92.0	–1.21	1.03
Total	1,800	242	23,266						

Table 5

Nissan Leaf AZE0 2014

Weight, kg	P_v	1,498
Maximum load capacity, kg		
Wheel base, m	$l_{vf}+l_{vr}$	2.7
	l_{vr}	1.17
	l_{vf}	1.53
Frontal effective area, m^2	S_{ve}	2.27
Wheel radius, m	r_d	0.3162
Height of application of wind force, m	h_w	0.75

Table 6

Results of calculations according to formula (20) for the WLTP Class 3b test cycle

θ°	max	Low 3	Medium 3-2	High 3-2	Extra-High -3
0	0.42	0.1767	0.1782	0.1822	0.1214
5	0.4184	0.2629	0.2644	0.2684	0.2076
10	0.4136	0.3483	0.3498	0.3538	0.293
15	0.406	0.4321	0.4336	0.4376	0.3768
17	0.401	0.4651	0.4666	0.4666	0.4098

sures the determination of the angle of inclination, and calculate the amount of work on the ascent and descent according to the average data of Table 7. To do this, depending on the angle of inclination of the road and the driving mode, select the average value of the force from Table 7 and multiply it by the length of the segment of the path with the given inclination. At the end, sum up the results for all segments.

If there are several routes from point "A" to point "B", then the one that is shorter in length should be considered the best, but the one that consumes less energy.

Example. Consider the traffic routes between the two points presented in Fig. 7. We will compare only routes with the same length (M1 and M2).

Each of the considered routes has an original topology (Fig. 8).

Since the movement will take place in the city mode, we will use the "Low3+Medium 3-2" mode for calculations. For absolutely dry weather with maximum traction of the tires on the road and in the absence of wind, we get the results of the calculations presented in Fig. 9 and in Table 8. Fig. 9 shows in red the segment of the path in the recuperative mode of the electric vehicle.

The results of the calculations show that on the route "M1" the consumption of mechanical energy is greater compared to the route "M2". However, if the recuperation mode is fully used for the generation of electrical energy, it is possible to reduce the mechanical energy consumption by 1,029 kJ without taking into account the efficiency of the double energy conversion.

Each of the considered routes has an original topology (Fig. 8).

Conclusions. After evaluating the complete picture of forces acting on the electric vehicle during its uphill and downhill movement, and evaluating the degree of influence of each of the forces on mechanical energy consumption, taking into account the specified initial conditions, when performing the standardized test cycle WLTC class 3b, conclusions were drawn based on the results of the simulation:

1. For any electric vehicle, it is necessary to be able to calculate the mechanical energy spent on overcoming the forces of movement resistance. This approach makes it possible to separate from the features of the transmission of the driving torque to the wheels from the electric drive, its type, design, features of the accumulation of electrical energy, methods of recuperation, etc.

2. The topology of the route of the electric vehicle is important due to the features of the electric drive to ensure the recovery of a certain part of the kinetic energy during braking or when moving downhill.

3. Calculations of the mechanical operation of an electric vehicle must be carried out taking into account the driving mode, namely, taking into account the accelerations and decelerations that occur on its way. At the same time, the period

Table 7

Specific mechanical energy of an electric vehicle Nissan Leaf AZE0 depending on the road angle in the modes of the WLTC test cycle, class 3b

	Total		High+Extra		Low+Middle		Low		Middle		High		Extra-High	
θ°	A_U	A_D	A_U	A_D	A_U	A_D	A_U	A_D	A_U	A_D	A_U	A_D	A_U	A_D
degrees	kJ/m	kJ/m	kJ/m	kJ/m	kJ/m	kJ/m	kJ/m	kJ/m	kJ/m	kJ/m	kJ/m	kJ/m	kJ/m	kJ/m
0	0.8	0.8	0.8	0.8	0.7	0.7	0.7	0.7	0.7	0.7	0.7	0.7	0.9	0.9
1	1.1	0.4	1.1	0.5	1.1	0.4	1.1	0.4	1.0	0.4	1.1	0.4	1.2	0.5
2	1.4	0.1	1.5	0.1	1.4	0.0	1.5	0.0	1.4	0.0	1.4	0.0	1.5	0.2
3	1.8	–0.2	1.8	–0.2	1.7	–0.3	1.8	–0.3	1.7	–0.3	1.8	–0.3	1.9	–0.1
4	2.1	–0.6	2.1	–0.6	2.1	–0.6	2.2	–0.7	2.0	–0.6	2.1	–0.7	2.2	–0.5
5	2.5	–0.9	2.5	–0.9	2.4	–1.0	2.5	–1.0	2.4	–0.9	2.4	–1.0	2.5	–0.8
6	2.8	–1.3	2.8	–1.2	2.8	–1.3	2.9	–1.4	2.7	–1.3	2.8	–1.4	2.8	–1.1
7	3.1	–1.6	3.2	–1.6	3.1	–1.7	3.2	–1.8	3.0	–1.6	3.1	–1.7	3.2	–1.5
8	3.5	–1.9	3.5	–1.9	3.5	–2.0	3.6	–2.1	3.4	–2.0	3.5	–2.1	3.5	–1.8
9	3.8	–2.3	3.8	–2.3	3.8	–2.4	3.9	–2.5	3.7	–2.3	3.8	–2.4	3.8	–2.1
10	4.1	–2.6	4.2	–2.6	4.1	–2.7	4.3	–2.8	4.0	–2.6	4.2	–2.7	4.1	–2.4
11	4.5	–3.0	4.5	–2.9	4.5	–3.0	4.7	–3.2	4.3	–2.9	4.5	–3.1	4.5	–2.8
12	4.8	–3.3	4.8	–3.2	4.8	–3.4	5.0	–3.6	4.7	–3.3	4.8	–3.4	4.8	–3.1
13	5.1	–3.6	5.1	–3.6	5.1	–3.7	5.4	–3.9	5.0	–3.6	5.2	–3.8	5.1	–3.4
14	5.5	–4.0	5.5	–3.9	5.5	–4.1	5.7	–4.2	5.3	–3.9	5.5	–4.1	5.4	–3.8
15	5.8	–4.3	5.8	–4.2	5.8	–4.4	6.0	–4.6	5.6	–4.2	5.8	–4.4	5.7	–4.1
16	6.1	–4.6	6.1	–4.6	6.1	–4.7	6.4	–4.9	6.0	–4.6	6.2	–4.8	6.1	–4.4
17	6.4	–5.0	6.4	–4.9	6.4	–5.0	6.7	–5.3	6.3	–4.9	6.5	–5.1	6.4	–4.7
18	6.8	–5.3	6.8	–5.2	6.8	–5.4	7.0	–5.6	6.6	–5.2	6.8	–5.4	6.7	–5.0
19	7.1	–5.6	7.1	–5.6	7.1	–5.7	7.4	–6.0	6.9	–5.5	7.1	–5.8	7.0	–5.4
20	7.4	–5.9	7.4	–5.9	7.4	–6.0	7.7	–6.3	7.2	–5.8	7.5	–6.1	7.3	–5.7

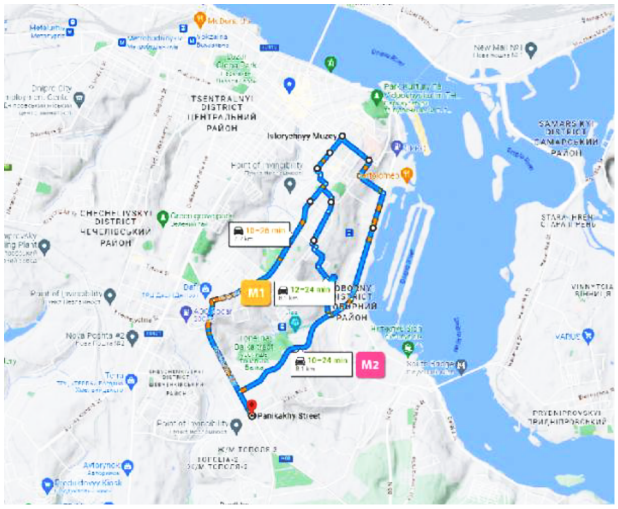

Fig. 7. Traffic routes M1 and M2 [20]

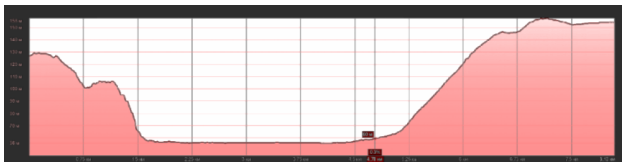

a

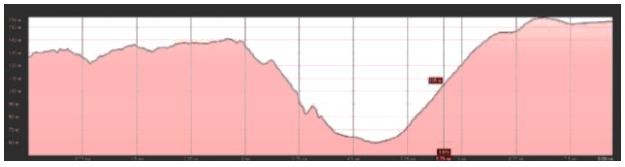

b

Fig. 8. Topology of traffic routes [21]:
a – route M1; b – route M2

of pauses (stationary state) is an advantage for an electric vehicle over traditional ones due to the fact that there is no electrical energy during idle operation (if additional comfort options are not taken into account).

4. The driving mode of an electric vehicle is influenced by many factors, in particular: traffic interchanges, intersections, topology, traffic jams, as well as the driver's driving style. Therefore, to estimate the consumption of primary energy (for traditional vehicles) or electricity for electric vehicles, different test cycles, considered earlier, are used. The WLTC, class 3b test cycle is the most relevant to date for our purposes due to the fact that it has several stages of speed mode and acceleration and braking modes. Using a combination of these stages, you can approximately simulate one or another mode of movement.

5. Modeling based on the proposed methodology of ensuring the requisite mechanical traction force for the Nissan Leaf AZE0 electric vehicle, even under ideal dry weather conditions, elucidates that the feasibility of completing specific segments of the WLTP Class 3b cycle diminishes beyond an incline of 10°, with an incline of 17° emerging as critical across all segments. At this threshold, the maximum attainable traction force of the Nissan Leaf AZE0 electric vehicle falls short of the necessary force to overcome resistance forces impeding movement. Evidently, analogous challenges persist for other electric vehicle variants, hybrid versions of vehicles, or classic vehicles, warranting commensurate computational analyses.

6. The conditions for providing the necessary mechanical traction force deteriorate in proportion to the decrease in the friction coefficient in accordance with Table 2.

7. The headwind velocity also impacts the expenditure of mechanical energy. Calculations indicate that the portion of mechanical energy expended to overcome air resistance when wind speed varies from zero to 100 km/h ranges from 2 to 3 % up to 11 to 12 %. This constitutes a significant component that must be taken into account in calculations.

8. The amount of potential energy that can be regenerated far exceeds the capabilities of the electric drive and battery system of an electric vehicle. This necessitates considerable attention to addressing the complex issue of creating energy storage systems with a rapid means of obtaining regenerated electrical energy. Particularly, electric drive systems with supercapacitors may have a substantial advantage in this regard, but they are not in demand due to their high price. Users fail to consider the difference in operational expenses, which could be fairly quickly compensated.

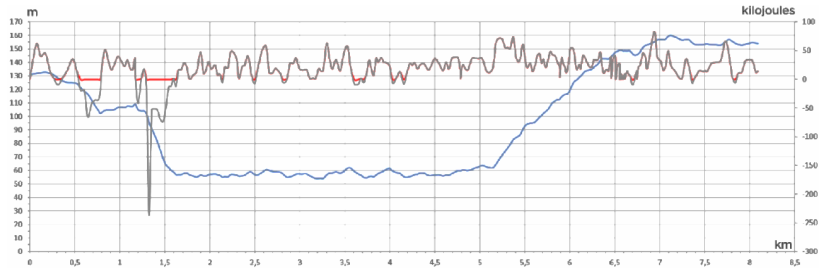

a

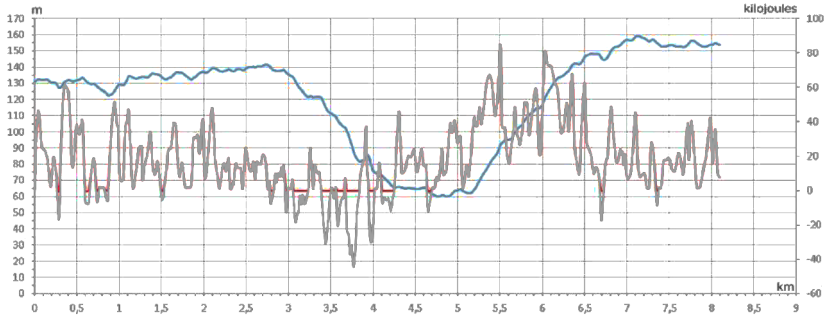

b

Fig. 9. Calculation results:
a – route M1; b – route M2

Table 8

Mechanical work on routes M1 and M2

	Work without taking into account recuperation, kJ	Work taking into account recuperation, kJ
M1	5,927.1	4,898.2
M2	5,787.11	5,068.6

9. The proposed methodology for calculating the mechanical work of an electric vehicle enables the selection of the most economical route to the destination from various options, thereby increasing the distance between battery charges and reducing the number of charging cycles.

References.

1. Jiao, Z., Ma, J., Zhao, X., Zhang, K., Meng, D., & Li, X. (2022). Development of a Rapid Inspection Driving Cycle for Battery Electric Vehicles Based on Operational Safety. *Sustainability, 14*, 5079. https://doi.org/10.3390/su14095079.

2. Egede, P., Dettmer, T., Herrmann, Ch., & Kara, S. (2015). Life Cycle Assessment of Electric Vehicles – A Framework to Consider Influencing Factors. *Procedia CIRP, 29*, 233-238. https://doi.org/10.1016/j.procir.2015.02.185.

3. Zaini, Z. (2020). Braking control strategies of modern hybrid and electric vehicles. *Journal of Physics: Conference Series, 1469*, 012173. https://doi.org/10.1088/1742-6596/1469/1/012173.

4. Jimenez Bermejo, D., Hernandez, S., Fraile-Ardanuy, J., Serrano Romero, J., Pozo, R., & Alvarez, F. (2018). Modelling the Effect of Driving Events on Electrical Vehicle Energy Consumption Using Inertial Sensors in Smartphones. *Energies, 11*, 412. https://doi.org/10.3390/en11020412.

5. Qi, X., Wu, G., Boriboonsomsin, K., & Barth, M. (2017). Data-driven decomposition analysis and estimation of link-level electric vehicle energy consumption under real-world traffic conditions. *Transportation Research Part D: Transport and Environment,* 64. https://doi.org/10.1016/j.trd.2017.08.008.

6. DieselNet (2019). *Worldwide Harmonized Light Vehicles Test Cycle (WLTC)*. Retrieved from https://dieselnet.com/standards/cycles/wltp.php.

7. Tutuianu, M., Bonnel, P., Ciuffo, B., Haniu, T., Ichikawa, N., Marotta, A., Pavlovic, J., & Steven, H. (2015). Development of the World-wide harmonized Light duty Test Cycle (WLTC) and a possible pathway for its introduction in the European legislation. *Transportation Research Part D Transport and Environment, 40*, 61-75. https://doi.org/10.1016/j.trd.2015.07.011.

8. UNECE (2005, April 1). *Global Technical Regulations (GTRs)*. Retrieved from https://unece.org/transport/standards/transport/vehicle-regulations-wp29/global-technical-regulations-gtrs.

9. Babangida, A., & Szemes, P. T. (2021). Electric Vehicle Modelling and Simulation of a Light Commercial Vehicle Using PMSM Propulsion. *Hungarian Journal of Industry and Chemistry, 49*(1), 37-46. https://doi.org/10.33927/HJIC-2021-06.

10. Choi, G., & Jahns, T. M. (2013). Design of electric machines for electric vehicles based on driving schedules. *2013 International Electric Machines & Drives Conference*, 54-61. https://doi.org/10.1109/IEMDC.2013.6556192.

11. Hayes, J., & Davis, K. (2014). *Simplified electric vehicle powertrain model for range and energy consumption based on EPA coast-down parameters and test validation by Argonne National Lab data on the Nissan Leaf*, 1-6. https://doi.org/10.1109/ITEC.2014.6861831.

12. Emadi, A. (Ed.) (2014). *Advanced Electric Drive Vehicles* (*1st* ed.). CRC Press. https://doi.org/10.1201/9781315215570.

13. Mediouni, H., Ezzouhri, A., Charouh, Z., El Harouri, K., El Hani, S., & Ghogho, M. (2022). Energy Consumption Prediction and Analysis for Electric Vehicles: A Hybrid Approach. *Energies, 15*, 6490. https://doi.org/10.3390/en15176490.

14. Kropiwnicki, J., & Furmanek, M. (2019). Analysis of the regenerative braking process for the urban traffic conditions. *Combustion Engines, 178*(3), 203-207. https://doi.org/10.19206/CE-2019-335.

15. Arat, M., & Bolarinwa, E. (2015). Rolling Resistance Effect of Tire Road Contact in Electric Vehicle Systems. *SAE Technical Papers*, 2015. https://doi.org/10.4271/2015-01-0624.

16. Vodovozov, V., Raud, Z., Lehtla, T., Rassõlkin, A., & Lillo, N. (2014). Comparative analysis of electric drives met for vehicle propulsion. *2014 9th International Conference on Ecological Vehicles and Renewable Energies, EVER 2014*, 1-8. https://doi.org/10.1109/EVER.2014.6844125.

17. Ben-Marzouk, M., Guy, C., Pelissier, S., Sari, A., & Venet, P. (2018). Determination of the electric vehicles driving modes in real life conditions by classification methods. *2018 IEEE International Conference on Industrial Technology (ICIT)*, 2060-2065. https://doi.org/10.1109/ICIT.2018.8352506.

18. Kravets, V., Ziborov, K., Bas, K., & Fedoriachenko, S. (2019). Combined method for determining the optimal flow distribution plan for mining, urban electric vehicles and for charging stations. *E3S Web of Conferences, 123*, 01029. https://doi.org/10.1051/e3sconf/201912301029.

19. Deng, Y., Lu, K., Liu, T., Wang, X., Shen, H., & Gong, J. (2023). Numerical Simulation of Aerodynamic Characteristics of Electric Vehicles with Battery Packs Mounted on Chassis. *World Electric Vehicle Journal, 26*. https://doi.org/10.3390/wevj14080216.

20. Google Maps (2024). *Dnipro, Dnipropetrovsk oblast, Ukraine*. Retrieved from https://www.google.com/maps/place/Dnipro,+Dnipropetrovsk+Oblast,+Ukraine.

21. Google Earth (2024). *Dnipro, Dnipropetrovsk oblast, Ukraine*. Retrieved from https://earth.google.com/web/@48.4501043,34.9830107,122.47063345a,36000d,35y,0h,0t,0r.

Витрати енергії електромобіля з урахуванням топології маршруту

О. С. Бешта[1], *О. О. Бешта*[1], *С. С. Худолій*[1], *Т. О. Халаімов*[*1], *В. С. Федорейко*[1]

1 – Національний технічний університет «Дніпровська політехніка», м. Дніпро, Україна

2 – Тернопільський національний педагогічний університет імені Володимира Гнатюка, м. Тернопіль, Україна

*Автор-кореспондент e-mail: khalaimov.ta.o@nmu.one

Мета. Визначення впливу фактору топології маршруту на витрати механічної роботи електромобіля – є головним завданням даної роботи. Вплив визначається за допомогою розрахунку витрат механічної роботи при русі електромобіля з урахуванням рекуперації енергії. Завдання також включає оцінку сил, що діють на електромобіль на прикладі Nissan Leaf AZEO 2014 року випуску.

Методика. У роботі використовується математична модель, що оцінює кількість механічної роботи, необхідної для подолання одного з обраних маршрутів, з урахуванням рекуперації енергії. Оцінка виконується за допомогою найбільш розповсюдженого стандартизованого циклу WLTC class 3b.

Результати. Результатом дослідження є розроблена математична модель, що дозволяє ефективно оцінити обсяг механічної роботи для подолання заданого маршруту й можливу енергію рекуперації. Запропонована методика дозволяє визначити найбільш економічний маршрут руху, із прокладених від початкової точки до пункту призначення, з урахуванням витрат механічної енергії.

Наукова новизна. Дано опис основних складових, що впливають на споживання електроенергії, з урахуванням повної картини сил, які діють на електромобіль під час руху.

Практична значимість. Отримані результати мають практичне значення для вибору найбільш оптимального маршруту руху електромобіля, що сприяє ефективному використанню енергії. Запропонована методика може бути використана на практиці для планування маршрутів з точки зору максимального енергозбереження.

Ключові слова: *електромобіль, топологія маршруту, рекуперація, оптимальний маршрут, енергетична ефективність, WLTC*

The manuscript was submitted 07.12.23.